Relationship between Landslides and Active Normal Faulting in the Epicentral Area of the AD 1556 *M*~8.5 Huaxian Earthquake, SE Weihe Graben (Central China)

Gang Rao [*1, 2], **Yali Cheng**[1], **Aiming Lin**[2], **Bing Yan**[2, 3]

1. *School of Earth Sciences, Zhejiang University, Hangzhou* 310027, *China*
2. *Department of Geophysics, Graduate School of Science, Kyoto University, Kyoto* 606-8502, *Japan*
3. *School of Earth Sciences and Engineering, Nanjing University, Nanjing* 210093, *China*

Gang Rao: http://orcid.org/0000-0003-3094-0311

ABSTRACT: In this paper, we focus on the characteristics of the landslides developed in the epicentral area of AD 1556 *M*~8.5 Huaxian Earthquake, and discuss their relations to the active normal faults in the SE Weihe Graben, Central China. The results from analyzing high-resolution remote-sensing imagery and digital elevation models (DEMs), in combination with field survey, demonstrate that: (i) the landslides observed in the study area range from small-scale debris/rock falls to large-scale rock avalanches; (ii) the landslides are mostly developed upon steep slopes of ≥30°; and (iii) the step-like normal-fault scarps along the range-fronts of the Huashan Mountains as well as the thick loess sediments in the Weinan area may facilitate the occurrence of large landslides. The results presented in this study would be helpful to assess the potential landslide hazards in densely-populated areas affected by active normal faulting.
KEY WORDS: landslides, active normal faults, Huaxian Earthquake, Weihe Graben, Ordos Block.

0 INTRODUCTION

Many factors may be responsible for the occurrence of landslides, such as moderate to large earthquakes (e.g., Tian et al., 2016; Xu et al., 2016; Ren et al., 2014a, b, 2013; Has et al., 2012; Dai et al., 2011a; Chigira et al., 2010; Ren and Lin, 2010; Owen et al., 2008; Harp and Jibson, 1996; Keefer, 1994, 1984), typhoons (e.g., Tsou et al., 2011; Fujisawa et al., 2010), as well as human activities (e.g., Huang and Chan, 2004; Barnard et al., 2001). Among them, earthquake-induced landslides particularly that within the epicentral areas of large earthquakes often caused serious damages and casualties within a distance of several to tens of kilometers (e.g., Meunier et al., 2008, 2007; Das et al., 2007; Dadson et al., 2004; Keefer, 2000; Jibson and Keefer, 1989). Previous studies also suggested that co-seismic landslides tend to be concentrated along co-seismic surface rupture zones which are usually controlled by active faults (e.g., Ren et al., 2014a; Dai et al., 2011b; Ren and Lin, 2010; Jibson et al., 2004). Therefore, investigations on the characteristics of the landslides in the epicentral areas of historical earthquakes and their relations to active faults are crucial for making an assessment of potential landslide hazards particularly that in densely-populated regions.

In this study, we investigate the characteristics of the landslides distributed in the epicentral area of the *M*~8.5 Huaxian Great Earthquake that occurred on January 23, 1556 (between Weinan and Huayin; Fig. 1). This earthquake caused serious damages and >830 000 deaths, including that resulted from co-seismic landslides (Yuan and Feng, 2010; CENC, 2007; Li and Cui, 2007; Xie, 1992; Kuo, 1957). On the basis of analyzing remote sensing images and DEMs, combined with field observations, we delineate the characteristics of the observed landslides (Fig. 2), and demonstrate the close relationship between the landslides and the active normal faulting. Finally, we discuss the implications for assessing potential landslide hazards in actively extending regions.

1 GEOLOGICAL BACKGROUND

The Weihe Graben in Central China (Fig. 1), is situated at the south margin of Ordos Block consisting of consolidate crystalline basement (SSB, 1988). To the south, it is bounded by the Qinling Mountains that were formed in association with the collision between the North China Craton (NCC) and the South China Block (SCB) in the Triassic (e.g., Ratschbacher et al., 2003; Meng and Zhang, 2000). As one of the Cenozoic graben systems developing around the Ordos Block, extensional deformation in the Weihe Graben started from the Eocene at ~50 Ma, resulting in >7 km thick sediments (Liu et al., 2013; Zhang et al., 1998; SSB, 1988).

The Huashan Mountains in the eastern part with a peak elevation of ~1 700 m above the sea level are mainly composed of pre-Mesozoic metamorphic basement rocks (SSB, 1988). A
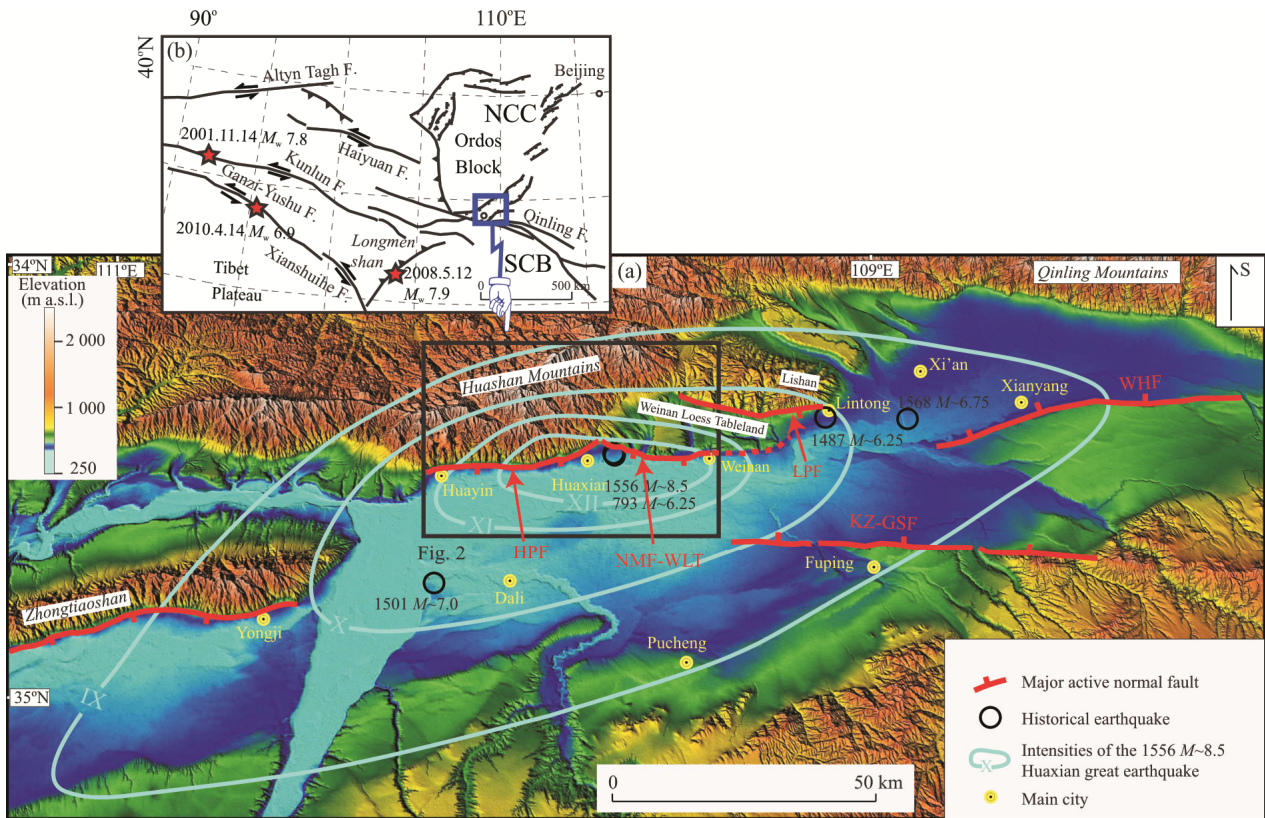
Rao, G., Cheng, Y. L., Lin, A. M., et al., 2017. Relationship between Landslides and Active Normal Faulting in the Epicentral Area of the AD 1556 *M*~8.5 Huaxian Earthquake, SE Weihe Graben (Central China). *Journal of Earth Science*, 28(3): 545–554. doi:10.1007/s12583-017-0900-z. http://en.earth-science.net

Figure 1. (a) Color-shaded relief map showing the topographic features of the eastern Weihe Graben. The major active fault traces are from Deng (2007). The historical earthquake data are from SEIN (2011). The intensity XII of the 1556 *M*~8.5 Huaxian Earthquake is the maximum in Chinese intensity scale. (b) The inset map shows the location of study area along the south margin of the Ordos Block. LPF. Lishan piedmont fault; NMF-WLT. northern margin fault of the Weinan Loess Tableland; HPF. Huashan piedmont fault; KZ-GSF. Kouzhen-Guanshan fault; WHF. Weihe fault; NZF. North Zhongtiaoshan fault; NCC. North China Craton; SCB. South China Block.
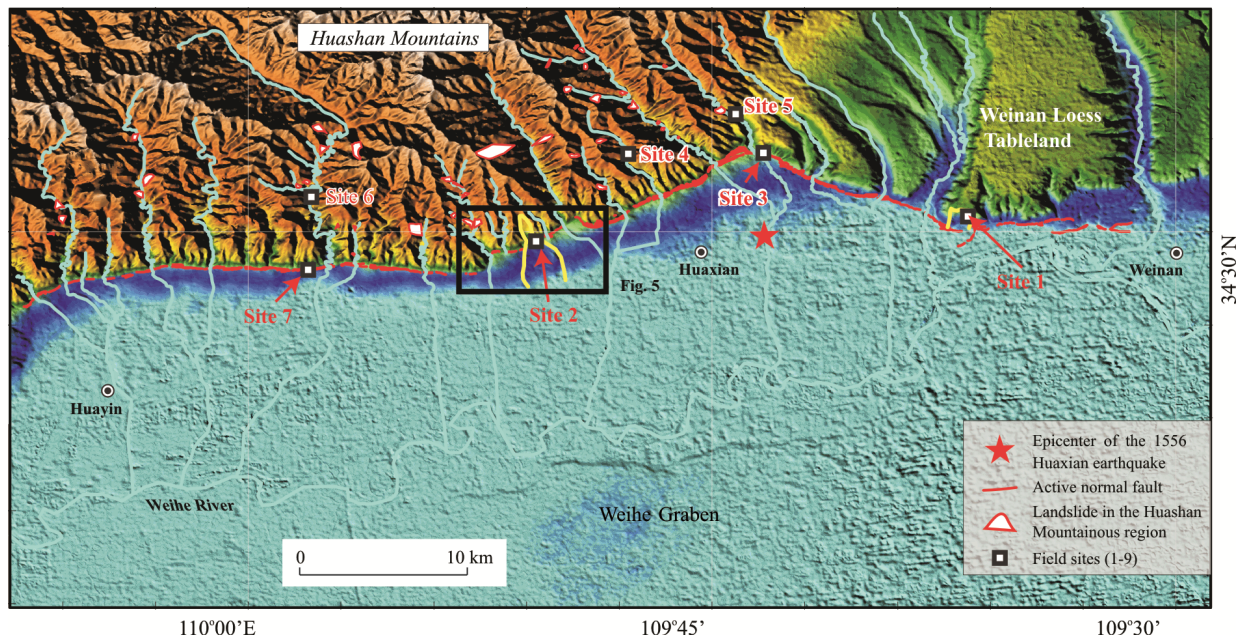

Figure 2. 3D perspective view (looking south) of SRTM DEM data showing the distribution of major landslides in the epicentral area of the Huaxian Great Earthquake between Huayin and Weinan cities. The vertical exaggeration (V.E.) is 3.

previous investigation based on fission track dating has demonstrated its uplift started at ~68.2 Ma, and the uplift-rate has accelerated to ~0.19 mm/yr since ~17.8 Ma (Yin et al., 2001).

To the west, the Weinan Loess Tableland is mainly composed of Quaternary alluvial deposits and >100 m-thick loess sediments (Fig. 1a; SSB, 1988), and was uplifted probably since

~1.2 Ma (Feng and Dai, 2004).

Several moderate to large historical earthquakes have occurred in the SE Weihe Graben, which can be dated back to BC 7 (Deng, 2007; SSB, 1988). In particular, previous studies have speculated the magnitude of the AD 1556 Huaxian Earthquake is as large as ~8.5, and inferred the region between Weinan and Huayin as the epicentral area according to the building damages and loss of people (Yuan and Feng, 2010; SSB, 1988). Major active faults include Huashan piedmont fault (HPF) and northern margin fault of the Weinan Loess Tableland (NMF-WLT) (Fig. 1a). They are both characterized by normal-slip motion with average throw-rates of ~1.5–3.0 mm/yr during the Late Pleistocene–Holocene (Rao et al., 2015, 2014; Deng et al., 2003; SSB, 1988; Li and Ran, 1983). Moreover, paleoseismological investigations demonstrate that Holocene surface-rupturing earthquakes have repeatedly occurred along these belts (Rao et al., 2015; Zhang et al., 1995; SSB, 1988; Xu et al., 1988).

2 DATA AND METHODS

In this study, 1-m IKONOS (Greek word for "image") and 0.5-m World View spatial-resolution satellite images were used to identify landslides. Between them, the World View as a relatively new satellite was launched in September 2007, which has an average revisit time of 1.7 days and is capable of collecting 0.5 m imagery over one million square kilometers per day (Digital Global, Inc., 2016).

Firstly, we mapped the extents of major landslides by integrating SRTM (shutter radar topography mission) DEMs (Figs. 3a and 4) with remote sensing images in perspective views (Figs. 3b and 5a). Then, we carried out fieldwork to observe the detailed characteristics of the landslides according to the distribution from our analysis (Figs. 3c–3e, 5b and 6b). Classifications of landslide types in this study are based on the guidebook provided by the U.S. Geological Survey (Highland and Bobrowsky, 2008). As slope morphology (particularly slope angle) may play significant roles in controlling landslide development (e.g., Ren and Lin, 2010; Chuang et al., 2009; Owen et al., 2008), topographic analysis was also carried out based on DEMs (Fig. 8). Finally, in combination with the features of active normal fault zones observed in the field, we
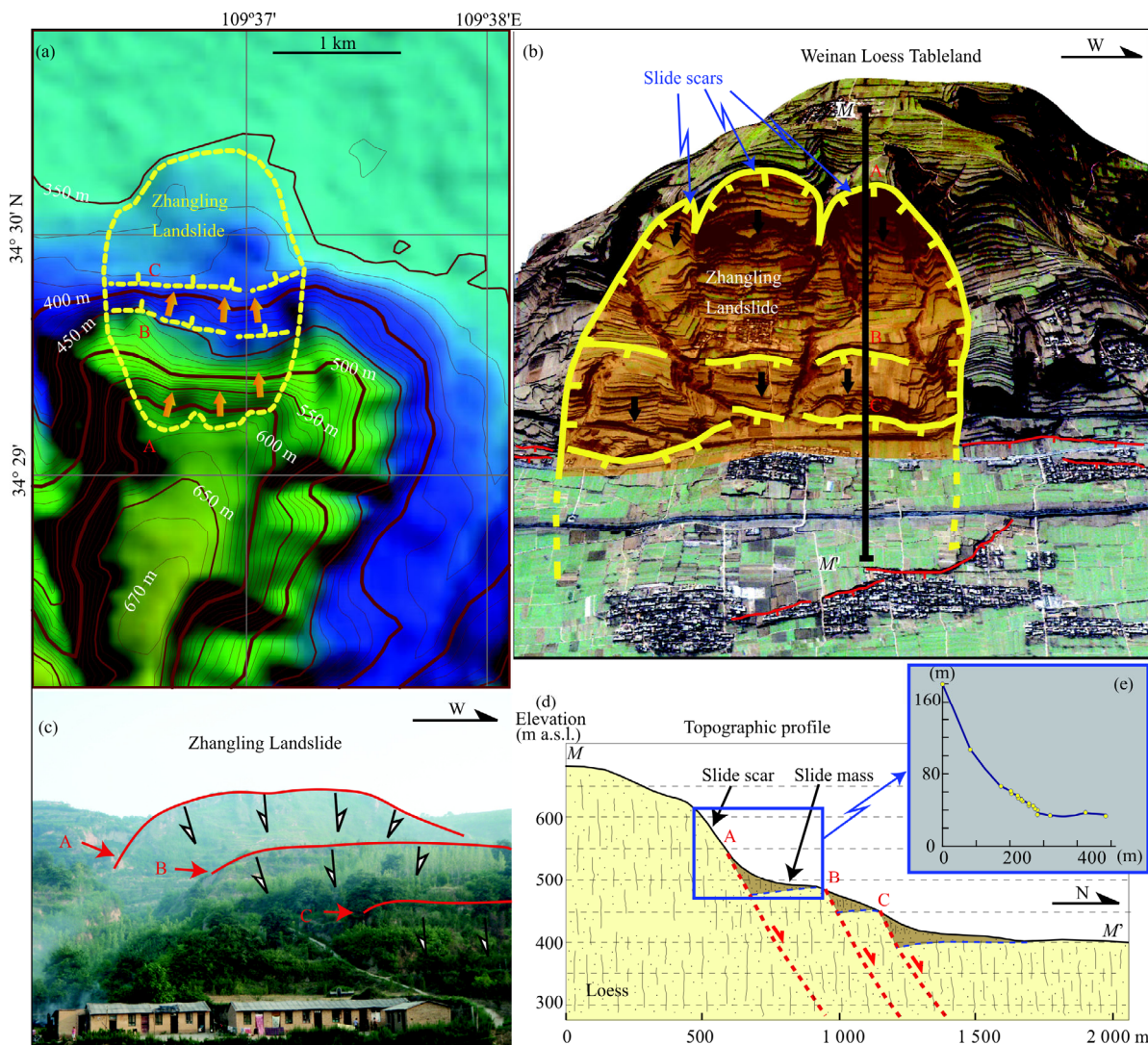

Figure 3. (a) Color-shaded relief map and (b) 3D perspective view (looking south) of IKONOS image reveal the extent of Zhangling Landslide (Site 1 in Fig. 2). (c) The interpreted arc-shaped slide scars (A) and inner scarps (B and C) observed in the field. The profiles generated from DEMs (d) and measured by using the laser rangefinder (e) demonstrate the topographic characteristics in detail.
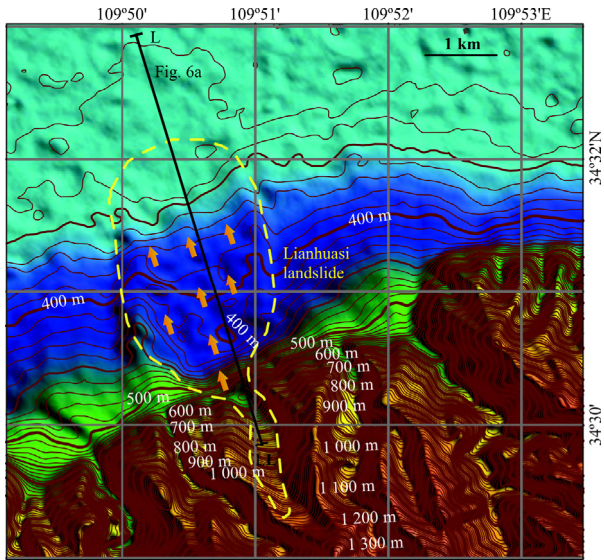
Figure 4. Color-shaded relief map showing the extent and slide direction of the Lianhuasi Landslide.

discussed the relationship between the landslides and the active normal faulting (Figs. 9 and 10). All the remote sensing images and DEMs were processed by using ENVI software, including 3D interpretations and topographic analysis.
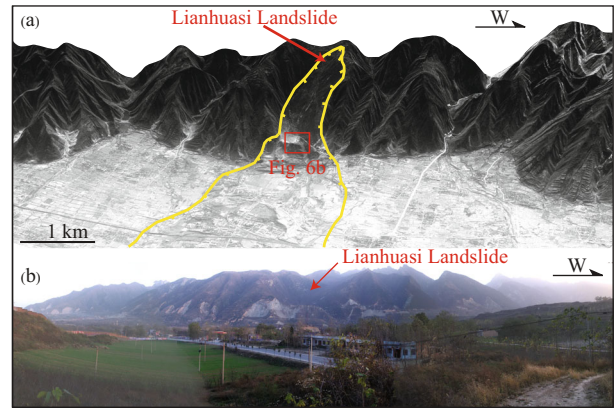

Figure 5. (a) World view of 0.5-m resolution image along the range-front of Huashan Mountains. V.E.=5. (b) Panoramic photograph reveals the largest Lianhuasi Landslide developed.

3 DISTRIBUTION AND CHARACTERISTICS

In the study area, large-volume landslides including the Zhangling and Lianhuasi landslides are pronounced along the northern margins of Weinan Loess Tableland and Huashan Mountains, respectively (Fig. 2). Besides, landslides have also been identified in mountainous regions. The characteristics are described in detail as below.
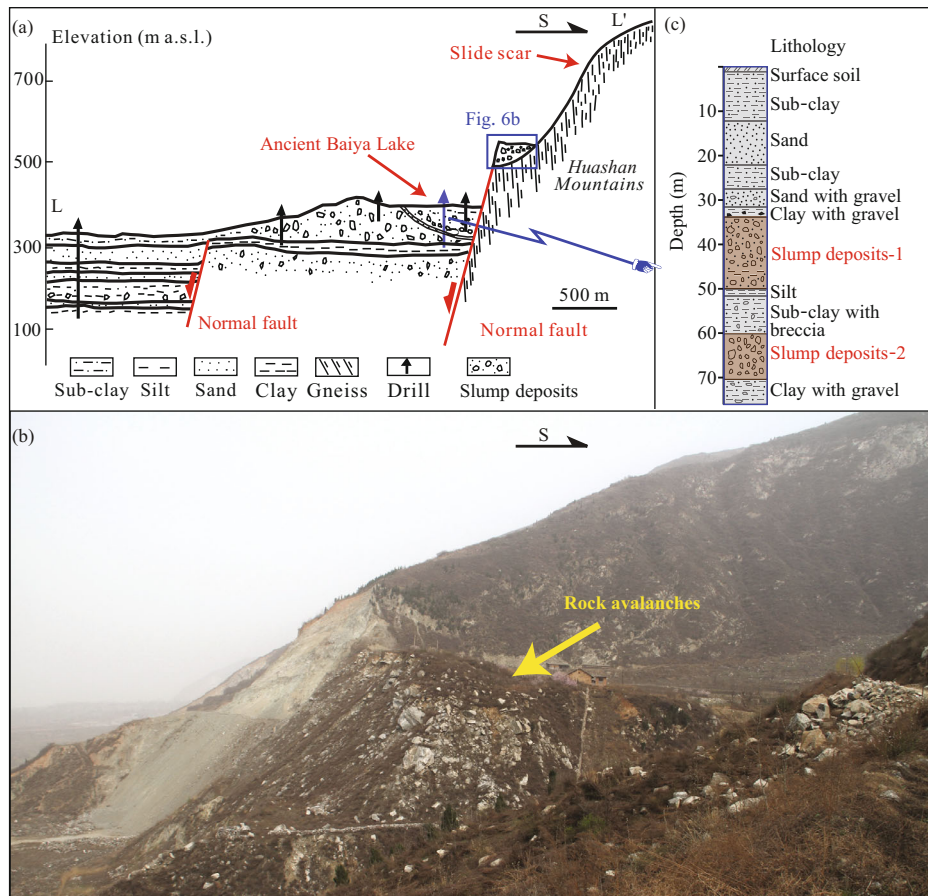

Figure 6. (a) Geological section reveals the landslide masses deposited across the active normal fault zone (drawn from SSB (1988)). (b) Rock avalanches observed in the field (Site 2 in Fig. 2). (c) The core-drilled data from ancient Baiya Lake demonstrate 2 layers of slump deposits (mainly sandy gravels) are intercalated with the contrasting lacustrine sediments (clay) (drawn from SSB (1988)), indicating the landslides probably repeatedly occurred at this site.

3.1 Zhangling Landslide

The Zhangling Landslide is located at Site 1, ~15 km east to the Weinan City (Fig. 2), which is the largest landslide in the loess area. The northward protuberance of topography characterizes the color-shaded relief map (Fig. 3a), revealing the approximate extent of this landslide. Detailed analysis demonstrates the arc-shaped slide scar (A) and two sets of inner scarps (B and C), and a conservative slide-area of ~2.75 km^2 is estimated (Fig. 3a). These characteristics are especially pronounced from a perspective view of the 1-m IKONOS image (Fig. 3b), which can also be observed in the field (Fig. 3c). The morphology of the slide scars and the masses re-deposited at the rear of individual slides are evident on the topographic profiles constructed from DEMs (Fig. 3d) and that measured in the field (Fig. 3e).

3.2 Lianhuasi Landslide

At Site 2, DEMs and 0.5-m World View image reveal the slide-area of Lianhuasi Landslide is >6 km^2 and the run-out distance reaches ~4 km from its main scar (Figs. 4 and 5a). Even if the range-fronts have been modified by modern quarrying, the morphology of the slide scar is still pronounced (Fig. 5b). It is the largest landslide mapped along the Huashan piedmont, where the slide masses characterized by large-scale rock avalanches are widely distributed and still can be observed in the field (Figs. 6a and 6b). Moreover, at least 2 layers of slump deposits (consisting of sandy gravels) intercalated with the lacustrine sediments (clay) were identified from the core-drillings acquired in ancient Baiya Lake (Fig. 6c; SSB, 1988), revealing the probably repeated occurrence of landslides at this site.

3.3 Other Landslides

Other landslides have also been mapped from remote sensing images, such as that observed at Site 3. The observed landslide is <500 m^2, and is featured by rock/debris falls along the margin of uplifted fluvial and loess sediments (Fig. 7a). It is worthy to note that quarrying along the range-fronts of the Huashan Mountains as shown in Fig. 5, has contributed to and/or aggravated the landslide development. In the mountainous regions, however, it is easier to map the slope failure along river valleys with slide-areas of 0.007–0.196 km^2 (Table 1), including rock falls, rockslide and topple (Figs. 7b–7d; see Fig. 2 for the locations).

4 SLOPE ANALYSIS

Based on the DEMs the results of our analysis indicate that higher slope values as much as 65º characterize the Huashan Mountains, whereas the low-lying Weihe Graben is almost flat with much gentler slopes (Fig. 8a). Differences are also obvious if we see from the profiles. In contrast to the highly rugged mountainous regions, slopes in the basin area are mostly <10$^°$ (Fig. 8b). The topographic transition zone along the basin boundary with slopes of 30º–52º (Fig. 8b), is the place where the giant landslides occurred (e.g., Lianhuasi Landslide; Figs. 4–6). Since the range fronts have been strongly modified by modern human activity (mostly quarrying), we analyzed the slopes of the landslides identified in the Huashan Mountains. As shown in Fig. 8c, all the slopes upon which landslides occurred are steep with angles of ≥40$^°$.

5 DISCUSSION

5.1 Relationship between Landslides and Active Normal Faulting

Remote sensing interpretations and topographic analysis demonstrate that the observed landslides are mostly developed along the steep inner valleys of the Huashan Mountains (≥40º; Fig. 8c), and along the north margin zones (e.g., Lianhuasi Landslide). This results are consistent with the slope morphologies of the landslides produced by the tectonic thrusting (e.g., Ren and Lin, 2010; Owen et al., 2008), and strike-slip faulting (e.g., Xu and Xu, 2014; Xu et al., 2013). Meanwhile, the topographic transition zone corresponds to the active normal-fault zones, which are characterized by step-like fault scarps with steep faults as observed in the field (Fig. 9). Both the field mapping and the numeral modelling suggested that step-like slopes could locally affect the seismic ground motion (topographic amplification), and consequently trigger intense progressive failures upon steep slopes (e.g., Alfaro et al., 2012; Lenti and Martino, 2012; Sepúlveda et al., 2005). Affected by active faulting, the rocks are strongly deformed and mostly consist of highly sheared and fractured rock masses (Fig. 9b). Due to tectonic weakening they would lose their internal cohesion and hence reduce their strengths, facilitating the occurrence of rock-slope failures (Dai et al., 2011b; Korup, 2004). Moreover, large-volume landslides (e.g., rock avalanches) are able to transport across the stepped slopes in active normal fault zones for long distances up to several kilometers (Fig. 10). Thus, we suggest the occurrence of landslides are facilitated by active normal faulting. Meanwhile, the relationship between the landslides and the stepped normal faults under tectonic extension demonstrated here provides a basis for comparing with other tectonic settings. The landslides produced by strike-slip faulting may be distributed symmetrically on both sides of surface rupture zones (e.g., Gorum et al., 2014; Xu and Xu, 2014), whereas more landslides are generated on the hanging wall than that on the footwall, and might be affected by the geometry of thrust faults (e.g., Xu et al., 2015, 2014, 2013; Wang et al., 2002).

5.2 Implications for the Potential Landslide Hazards

During earthquakes, large portions of damages and casualties were caused by seismic-induced landslides, and moreover some of large landslides tend to recur in the same places (Soloneko, 1977). Thus, studies on characteristics of major landslides particularly that in epicentral areas of historical earthquakes are important keys to assess the landslide potential. In the study area, the Lianhuasi Landslide along the Huashan piedmont is the largest one, which was previously inferred to be triggered by the AD 1556 earthquake (Figs. 5–7; Yuan and Feng, 2010; Li and Cui, 2007; SSB, 1988). However, based on re-analysis of historical documents Zhou (2010) suggested the AD 1072 earthquake probably caused the Lianhuasi Landslide. By contrast, a recent OSL (optical stimulated luminescence) dating of the loess sediments covering the slide-related breccias delineated it was likely formed before 187 kyr ago (Du et al., 2013). Actually, to precisely bracket the timing of a paleo-slide and even to establish its seismic origin are often difficult (Jibson, 2009; Jibson and Keefer,

1993). But, at least it provides us a picture of the partial effects of a possible earthquake on the Huashan piedmont fault, which has been considered to be active and capable of generating large earthquakes (Rao et al., 2014; Zhang et al., 1995; SSB, 1988; Xu et al., 1988).

Meanwhile, we suggest attention should also be paid to the Weinan area where the thickness of loess sediments is >100 m (Figs. 1 and 2). It is fit for the occurrence of a giant loess landslide (e.g., Derbysgire, 2001; Soloneko, 1977). The size could be similar to the Zhangling Landslide which was suggested to be produced by the AD 1556 Huaxian Earthquake according to its location and morphological features recorded by historical documents (Fig. 3; Yuan and Feng, 2010; SSB, 1988; He, 1986). The potential hazards might be comparable

Table 1 Inventory of the landslides analyzed in this study

| Number	Lat. (°N)	Lon. (°E)	Area (km^2)	Slope (°)	Descriptions
1	34.500 658	110.106 451	0.019	50	Huangpuyu Valley
2	34.485 678	110.101 076	0.098	58	Huangpuyu Valley
3	34.495 386	110.096 686	0.095	45	Huangpuyu Valley
4	34.479 666	110.058 986	0.098	53	Xiaoyu Valley
5	34.470 842	110.053 420	0.196	45	Xiaoyu Valley
6	34.450 414	110.060 230	0.096	44	Xiaoyu Valley
7	34.492 384	109.967 368	0.083	47	Dafuyu Valley
8	34.475 623	109.973 165	0.042	55	Dafuyu Valley
9	34.474 180	109.968 055	0.044	60	Dafuyu Valley
10	34.458 015	109.960 097	0.120	44	Dafuyu Valley
11	34.444 419	109.960 513	0.195	60	Dafuyu Valley
12	34.497 105	109.951 892	0.020	62	Dafuyu Valley
13	34.456 035	109.942 727	0.146	52	Dafuyu Valley
14	34.512 057	109.943 538	0.027	57	Liuyu Valley
15	34.497 669	109.942 689	0.026	48	Liuyu Valley
16	34.499 654	109.912 179	0.124	51	Fangshanyu Valley
17	34.497 010	109.878 802	0.110	45	Gouyu Valley
18	34.490 401	109.889 377	0.059	47	Gouyu Valley
19	34.480 156	109.882 767	0.051	55	Gouyu Valley
20	34.473 878	109.886 072	0.046	52	Gouyu Valley
21	34.471 234	109.893 012	0.068	43	Gouyu Valley
22	34.493 706	109.876 489	0.106	50	Gouyu Valley
23	34.454 710	109.867 896	0.164	48	Xiaofuyu Valley
24	34.449 423	109.840 467	0.085	52	Xiaofuyu Valley
25	34.476 191	109.808 081	0.058	48	Tanyu Valley
26	34.459 363	109.825 820	0.058	47	Tanyu Valley
27	34.451 471	109.811 597	0.038	53	Taipingyu Valley
28	34.449 471	109.768 087	0.007	41	Shidiyu Valley
29	34.441 549	109.779 447	0.031	46	Shidiyu Valley
30	34.444 864	109.776 950	0.028	47	Shidiyu Valley
31	34.433 230	109.794 863	0.128	50	Shidiyu Valley
32	34.425 055	109.798 490	0.056	64	Shidiyu Valley
33	34.428 818	109.813 597	0.051	56	Shidiyu Valley
34	34.423 601	109.828 299	0.022	50	Shidiyu Valley
35	34.408 114	109.836 832	0.029	44	Shidiyu Valley
36	34.412 410	109.818 326	0.013	52	Shidiyu Valley
37	34.402 534	109.820 423	0.030	40	Shidiyu Valley
38	34.400 980	109.823 398	0.026	42	Shidiyu Valley
39	34.435 092	109.746 781	0.042	45	Mayu Valley
40	34.411 387	109.775 551	0.019	42	Mayu Valley
41	34.505 812	109.847 340	>6	45	Lianhuasi Landslide
42	34.495 925	109.616 827	~2.75	48	Zhangling Landslide
43	34.457 308	109.725 226	0.000 4	35	Weinan Loess margin
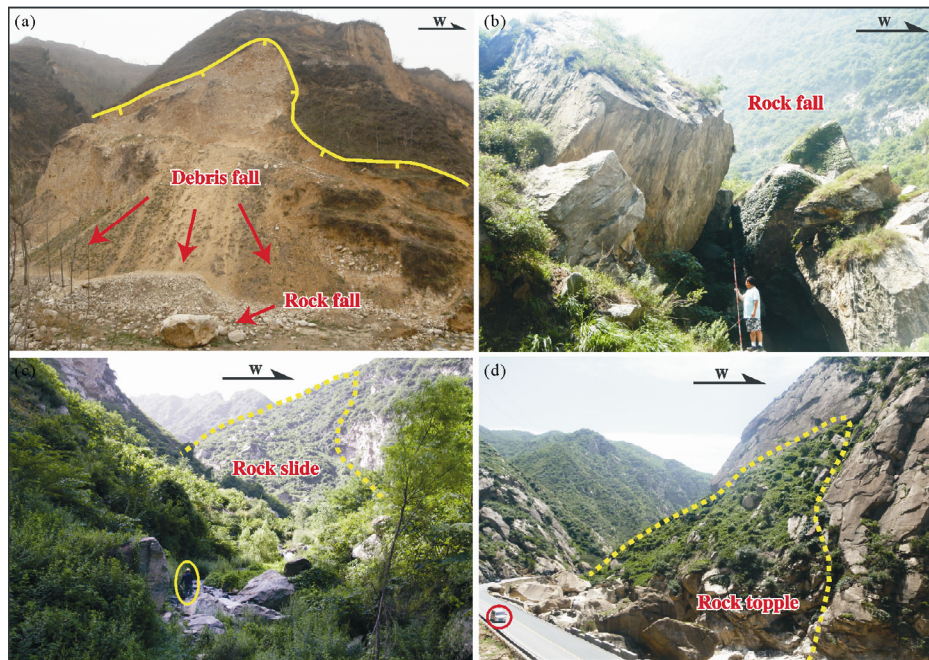
Figure 7. (a) Debris and rock falls observed at Site 3 along the northern margin of the Weinan Loess Tableland. (b) The rock fall, slide and topple observed in the Huashan mountainous regions ((b) Site 4; (c) Site 5; (d) Site 6 in Fig. 2).
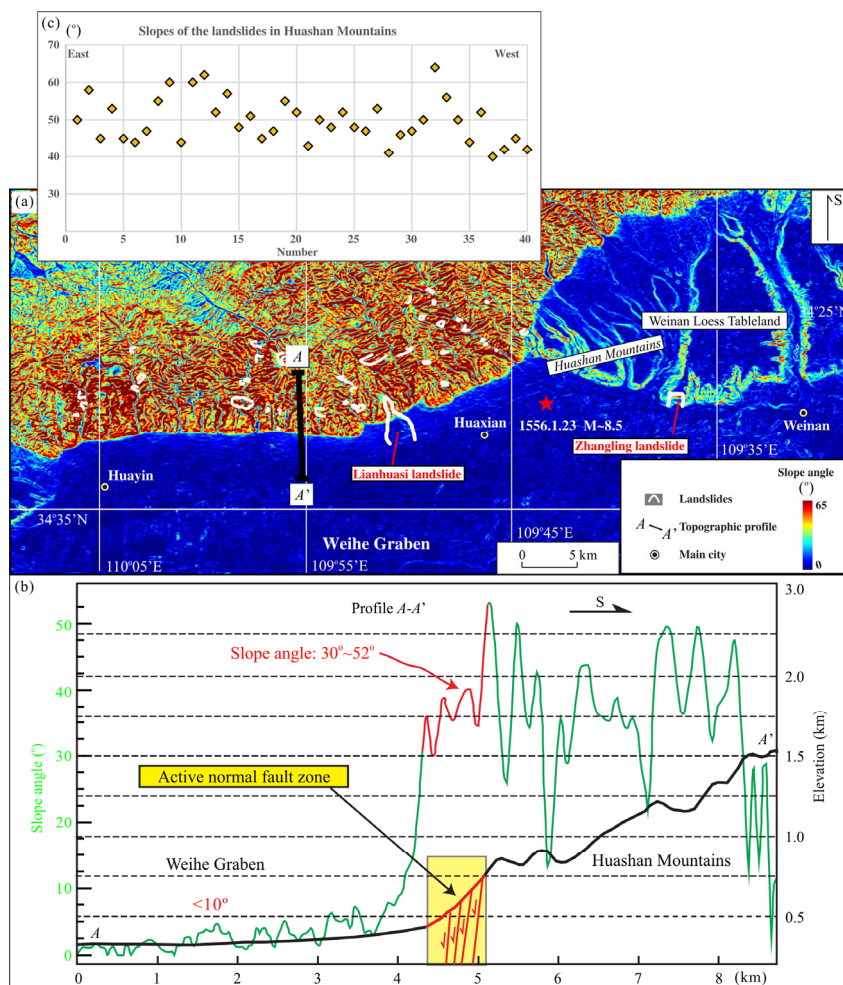

Figure 8. (a) Slope angle map indicates the contrasting topographic features between the Weihe Graben and the uplifted blocks including the Huashan and Weinan Loess Tableland; (b) steep slopes (as much as ~65°) characterize the mountainous area, whereas the low-lying flat Weihe Graben are mostly <10° in slope angle; (c) slope angles of the landslides in the Huashan Mountains.
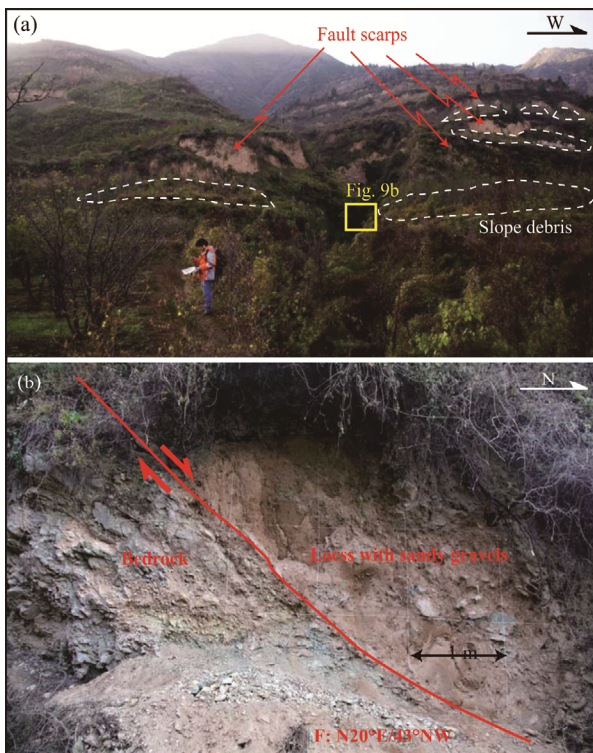
Figure 9. (a) Stepped normal-fault scarps observed along the Huashan piedmont (Site 7 in Fig. 2); (b) the exposed fault plane separating the fractured bedrock from the loess with sandy gravels.
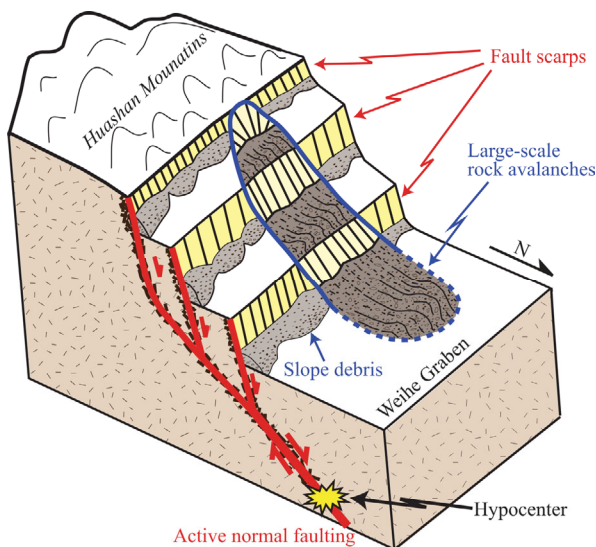

Figure 10. Schematic diagram showing the characteristics of the tectonic landforms affected by active normal faulting along the transition zone between Huashan and Weihe Graben. Meanwhile, the fault-generated step-like scarps facilitated the occurrence of the landslides.

with the landslides triggered by the AD 1920 *M* 8.5 Haiyuan Earthquake (Zhang and Wang, 2007; Close and McCormick, 1922). Therefore, it is particularly crucial for our study area, because it is densely populated and the historical seismicity was high. The results presented here may also be helpful to better understand the mechanism of gravity-driven movements (e.g., Gori et al., 2014; Carbonel et al., 2013; Moro et al., 2012), and how active normal faulting controls the landscape of range-

fronts in actively extending regions (e.g., Osmundsen et al., 2009; Densmore et al., 1998).

6 CONCLUSIONS

On the basis of analyzing remote sensing images and DEM data, combined with field observations, we have reached the following conclusions.

(i) The landslides observed in the study area range from small-scale debris/rock fall to large-scale rock avalanches.

(ii) The landslides are mostly developed upon steep slopes of ≥30°.

(iii) The step-like normal-fault scarps along the range-fronts of the Huashan Mountains as well as the thick loess sediments in Weinan area may facilitate the occurrence of large landslides.

REFERENCES CITED

Alfaro, P., Delgado, J., García-Tortosa, F. J., et al., 2012. Widespread Landslides Induced by the M_w 5.1 Earthquake of 11 May 2011 in Lorca, SE Spain. *Engineering Geology*, 137/138: 40–52. doi:10.1016/j.enggeo.2012.04.002

Barnard, P. L., Owen, L. A., Sharma, M. C., et al., 2001. Natural and Human-Induced Landsliding in the Garhwal Himalaya of Northern India. *Geomorphology*, 40(1/2): 21–35. doi:10.1016/s0169-555x(01)00035-6

Carbonel, D., Gutiérrez, F., Linares, R., et al., 2013. Differentiating between Gravitational and Tectonic Faults by Means of Geomorphological Mapping, Trenching and Geophysical Surveys: The Case of the Zenzano Fault (Iberian Chain, N Spain). *Geomorphology*, 189: 93–108. doi:10.1016/j.geomorph.2013.01.020

Chigira, M., Wu, X. Y., Inokuchi, T., et al., 2010. Landslides Induced by the 2008 Wenchuan Earthquake, Sichuan, China. *Geomorphology*, 118(3/4): 225–238. doi:10.1016/j.geomorph.2010.01.003

Chuang, S. C., Chen, H., Lin, G. W., et al., 2009. Increase in Basin Sediment Yield from Landslides in Storms Following Major Seismic Disturbance. *Engineering Geology*, 103(1/2): 59–65. doi:10.1016/j.enggeo.2008.08.001

CENC (China Earthquakes Network Center), 2007. The 1556 Huaxian Great Earthquake, Shaanxi, China: The Largest Total of Fatalities ever Claimed. [2016-03-15]. http://www.csi.ac.cn/manage/html/4028861611c5c2ba0111c5c558b00001/_history/hxz/qyzhenhai/zh20060609002.htm (in Chinese)

Close, U., McCormick, E., 1922. Where the Mountains Walked. *The National Geographic Magazin*e, 41: 445–472

Dadson, S. J., Hovius, N., Chen, H., et al., 2004. Earthquake-Triggered Increase in Sediment Delivery from an Active Mountain Belt. *Geology*, 32(8): 733. doi:10.1130/g20639.1

Dai, F. C., Xu, C., Yao, X., et al., 2011a. Spatial Distribution of Landslides Triggered by the 2008 *M*s 8.0 Wenchuan Earthquake, China. *Journal of Asian Earth Sciences*, 40(4): 883–895. doi:10.1016/j.jseaes.2010.04.010

Dai, F. C., Tu, X. B., Xu, C., et al., 2011b. Rock Avalanches Triggered by Oblique-Thrusting during the 12 May 2008 *M*s 8.0 Wenchuan Earthquake, China. *Geomorphology*, 132(3/4): 300–318. doi:10.1016/j.geomorph.2011.05.016

Das, J. D., Saraf, A. K., Panda, S., 2007. Satellite Data in a Rapid Analysis of Kashmir Earthquake (October 2005) Triggered Landslide Pattern and River Water Turbidity in and around the Epicentral Region. *International Journal of Remote Sensing*, 28(8): 1835–1842. doi:10.1080/01431160600954720

Deng, Q., 2007. Active Tectonics Map of China. Seismological Press, Beijing (in Chinese)

Deng, Q., Zhang, P., Ran, Y., et al., 2003. Basic Characteristics of Active Tectonics of China. *Science in China Series D*: *Earth Sciences*, 46: 356–372.

Densmore, A. L., Ellis, M. A., Anderson, R. S., 1998. Landsliding and the Evolution of Normal-Fault-Bounded Mountains. *Journal of Geophysical Research*: *Solid Earth*, 103(B7): 15203–15219. doi:10.1029/98jb00510

Derbyshire, E., 2001. Geological Hazards in Loess Terrain, with Particular Reference to the Loess Regions of China. *Earth-Science Reviews*, 54(1/2/3): 231–260. doi:10.1016/s0012-8252(01)00050-2

Digital Globe Inc., 2016. Content Collection/Satellites. [2016-03-15]. http://www.digitalglobe.com/about-us/content-collection#worldview-1

Du, J., Li, D., Ma, Y., et al., 2013. The High-Speed and Long-Distance Ancient Landslides before 187 ka: the Evidence from the OSL Dating of the Loess Overlying the Landslide Body of Lianhuasi Landslides in Huaxian, Shaanxi Province, China. *Quaternary Sciences*, 33: 1005–1015 (in Chinese with English Abstract)

Feng, X. J., Dai, W. Q., 2004. Lateral Migration of Fault Activity in Weihe Basin. *Acta Seismologica Sinica*, 17(2): 190–199. doi:10.1007/bf02896933

Fujisawa, K., Marcato, G., Nomura, Y., et al., 2010. Management of a Typhoon-Induced Landslide in Otomura (Japan). *Geomorphology*, 124(3/4): 150–156. doi:10.1016/j.geomorph.2010.09.027

Gori, S., Falcucci, E., Dramis, F., et al., 2014. Deep-Seated Gravitational Slope Deformation, Large-Scale Rock Failure, and Active Normal Faulting along Mt. Morrone (Sulmona Basin, Central Italy): Geomorphological and Paleoseismological Analyses. *Geomorphology*, 208: 88–101. doi:10.1016/j.geomorph.2013.11.017

Gorum, T., Korup, O., van Westen, C. J., et al., 2014. Why so Few? Landslides Triggered by the 2002 Denali Earthquake, Alaska. *Quaternary Science Reviews*, 95: 80–94. doi:10.1016/j.quascirev.2014.04.032

Harp, E. L., Jibson, R. W., 1996. Landslides Triggered by the 1994 Northridge, California, Earthquake. *Bulletin of Seismological Society of American*, 86: 319–332

Has, B., Noro, T., Maruyama, K., et al., 2012. Characteristics of Earthquake-Induced Landslides in a Heavy Snowfall Region—Landslides Triggered by the Northern Nagano Prefecture Earthquake, March 12, 2011, Japan. *Landslides*, 9(4): 539–546. doi:10.1007/s10346-012-0344-6

He, M., 1986. The Great 1556 Huaxian Earthquake and the Related Faulting. *Journal Seismological Research*, 9: 427–432 (in Chinese with English Abstract)

Highland, L. M., Bobrowsky, P., 2008. The Landslide Handbook—A Guide to Understanding Landslides. *U.S. Geological Survey Circular*, 1325: 129

Huang, R., Chan, L., 2004. Human-Induced Landslides in China: Mechanism Study and Its Implications on Slope Management. *Chinese Journal of Rock Mechanics and Engineering*, 23: 2766–2777

Jibson, R. W., 2009. Using Landslides for Paleoseismic Analysis. In: McCalpin, J. P., ed., Paleoseismology. *International Geophysical Series*, 95: 565–601

Jibson, R. W., Harp, E. L., Schulz, W., et al., 2004. Landslides Triggered by the 2002 Denali Fault, Alaska, Earthquake and the Inferred Nature of the Strong Shaking. *Earthquake Spectra*, 20(3): 669–691. doi:10.1193/1.1778173

Jibson, R. W., Keefer, D. K., 1993. Analysis of the Seismic Origin of Landslides: Examples from the New Madrid Seismic Zone. *Geological Society of America Bulletin*, 105(4): 521–536. doi:10.1130/0016-7606(1993)105<0521:aotsoo>2.3.co;2

Jibson, R. W., Keefer, D. K., 1989. Statistical Analysis of Factors Affecting Landslide Distribution in the New Madrid Seismic Zone, Tennessee and Kentucky. *Engineering Geology*, 27(1/2/3/4): 509–542. doi:10.1016/0013-7952(89)90044-6

Keefer, D. K., 2000. Statistical Analysis of an Earthquake-Induced Landslide Distribution—The 1989 Loma Prieta, California, Event. *Engineering Geology*, 58(3/4): 231–249. doi:10.1016/s0013-7952(00)00037-5

Keefer, D. K., 1994. The Importance of Earthquake-Induced Landslides to Long-Term Slope Erosion and Slope-Failure Hazards in Seismically Active Regions. *Geomorphology*, 10(1/2/3/4): 265–284. doi:10.1016/0169-555x(94)90021-3

Keefer, D. K., 1984. Landslides Caused by Earthquakes. *Geological Society of America Bulletin*, 95: 406–421

Korup, O., 2004. Geomorphic Implications of Fault Zone Weakening: Slope Instability along the Alpine Fault, South Westland to Fiordland. *New Zealand Journal of Geology and Geophysics*, 47(2): 257–267. doi:10.1080/00288306.2004.9515052

Kuo, T., 1957. On the Shensi Earthquake of January 23, 1556. *Acta Geophysica Sinica*, 6: 59–68 (in Chinese with English Abstract)

Lenti, L., Martino, S., 2012. The Interaction of Seismic Waves with Step-Like Slopes and Its Influence on Landslide Movements. *Engineering Geology*, 126: 19–36. doi:10.1016/j.enggeo.2011.12.002

Li, Z., Cui, P., 2007. The Secondary Disasters of Great Huaxian Earthquake in 1556. *Journal of Mountain Sciences*, 25: 425–430 (in Chinese with English Abstract)

Li, X., Ran, Y., 1983. Active Faults at Northern Front of the Huashan and Weinan Loess Tableland. *North China Earthquake Science*, 1: 10–18 (in Chinese with English Abstract)

Liu, J. H., Zhang, P. Z., Lease, R. O., et al., 2013. Eocene Onset and Late Miocene Acceleration of Cenozoic Intracontinental Extension in the North Qinling Range-Weihe Graben: Insights from Apatite Fission Track Thermochronology. *Tectonophysics*, 584: 281–296. doi:10.1016/j.tecto.2012.01.025

Meng, Q. R., Zhang, G. W., 2000. Geologic Framework and Tectonic Evolution of the Qinling Orogen, Central China. *Tectonophysics*, 323(3/4): 183–196. doi:10.1016/s0040-1951(00)00106-2

Meunier, P., Hovius, N., Haines, J. A., 2008. Topographic Site Effects and

the Location of Earthquake Induced Landslides. *Earth and Planetary Science Letters*, 275(3/4): 221–232. doi:10.1016/j.epsl.2008.07.020

Meunier, P., Hovius, N., Haines, A. J., 2007. Regional Patterns of Earthquake-Triggered Landslides and Their Relation to Ground Motion. *Geophysical Research Letters*, 34(20): L20408. doi:10.1029/2007gl031337

Moro, M., Saroli, M., Gori, S., et al., 2012. The Interaction between Active Normal Faulting and Large Scale Gravitational Mass Movements Revealed by Paleoseismological Techniques: A Case Study from Central Italy. *Geomorphology*, 151/152: 164–174. doi:10.1016/j.geomorph.2012.01.026

Osmundsen, P. T., Henderson, I., Lauknes, T. R., et al., 2009. Active Normal Fault Control on Landscape and Rock-Slope Failure in Northern Norway. *Geology*, 37(2): 135–138. doi:10.1130/g25208a.1

Owen, L. A., Kamp, U., Khattak, G. A., et al., 2008. Landslides Triggered by the 8 October 2005 Kashmir Earthquake. *Geomorphology*, 94(1/2): 1–9. doi:10.1016/j.geomorph.2007.04.007

Rao, G., Lin, A. M., Yan, B., 2015. Paleoseismic Study on Active Normal Faults in the Southeastern Weihe Graben, Central China. *Journal of Asian Earth Sciences*, 114: 212–225. doi:10.13039/501100001700

Rao, G., Lin, A. M., Yan, B., et al., 2014. Tectonic Activity and Structural Features of Active Intracontinental Normal Faults in the Weihe Graben, Central China. *Tectonophysics*, 636: 270–285. doi:10.13039/501100001700

Ratschbacher, L., Hacker, B. R., Calvert, A., et al., 2003. Tectonics of the Qinling (Central China): Tectonostratigraphy, Geochronology, and Deformation History. *Tectonophysics*, 366(1/2): 1–53. doi:10.1016/s0040-1951(03)00053-2

Ren, Z. K., Zhang, Z. Q., Dai, F. C., et al., 2014a. Topographic Changes Due to the 2008 M_w 7.9 Wenchuan Earthquake as Revealed by the Differential DEM Method. *Geomorphology*, 217: 122–130. doi:10.1016/j.geomorph.2014.04.020

Ren, Z. K., Zhang, Z. Q., Yin, J. H., et al., 2014b. Morphogenic Uncertainties of the 2008 Wenchuan Earthquake: Generating or Reducing?. *Journal of Earth Science*, 25(4): 668–675. doi:10.1007/s12583-014-0456-0

Ren, Z. K., Zhang, Z. Q., Dai, F. C., et al., 2013. Co-Seismic Landslide Topographic Analysis Based on Multi-Temporal DEM—A Case Study of the Wenchuan Earthquake. *Springer Plus*, 2(1): 544. doi:10.1186/2193-1801-2-544

Ren, Z. K., Lin, A. M., 2010. Co-Seismic Landslides Induced by the 2008 Wenchuan Magnitude 8.0 Earthquake, as Revealed by ALOS PRISM and AVNIR2 Imagery Data. *International Journal of Remote Sensing*, 31(13): 3479–3493. doi:10.1080/01431161003727770

Shaanxi Earthquake Information Network (SEIN), 2011. Historical Earthquakes in Shaanxi Province. [2016-03-15]. http://www.eqsn.gov.cn/manage/html/8abd83af1c88b3f2011c88b74299 001f/sxlsdz/index.html (in Chinese)

Sepúlveda, S. A., Murphy, W., Jibson, R. W., et al., 2005. Seismically Induced Rock Slope Failures Resulting from Topographic Amplification of Strong Ground Motions: The Case of Pacoima Canyon, California. *Engineering Geology*, 80(3/4): 336–348. doi:10.1016/j.enggeo.2005.07.004

Solonenko, V. P., 1977. Landslides and Collapses in Seismic Zones and Their Prediction. *Bulletin of the International Association of Engineering Geology*, 15(1): 4–8. doi:10.1007/bf02592633

State Seismological Bureau (SSB), 1988. Active Faults around the Ordos.

Seismological Press, Beijing. 335 (in Chinese)

Tian, Y. Y., Xu, C., Xu, X. W., et al., 2016. Detailed Inventory Mapping and Spatial Analyses to Landslides Induced by the 2013 *M*s 6.6 Minxian Earthquake of China. *Journal of Earth Science*, 27(6): 1016–1026. doi:10.1007/s12583-016-0905-z

Tsou, C. Y., Feng, Z. Y., Chigira, M., 2011. Catastrophic Landslide Induced by Typhoon Morakot, Shiaolin, Taiwan. *Geomorphology*, 127(3/4): 166–178. doi:10.1016/j.geomorph.2010.12.013

Wang, W. N., Nakamura, H., Tsuchiya, S., et al., 2002. Distributions of Landslides Triggered by the Chi-Chi Earthquake in Central Taiwan on September 21, 1999. *Landslides*, 38(4): 318–326. doi:10.3313/jls1964.38.4_318

Xie, Y., 1992. On Magnitude of 1556 Guanzhong Great Earthquake. *Journal of Catastrophology*, 7: 10–13 (in Chinese with English Abstract)

Xu, C., Xu, X. W., Tian, Y. Y., et al., 2016. Two Comparable Earthquakes Produced Greatly Different Coseismic Landslides: The 2015 Gorkha, Nepal and 2008 Wenchuan, China Events. *Journal of Earth Science*, 27(6): 1008–1015. doi:10.1007/s12583-016-0684-6

Xu, C., Xu, X. W., Yu, G. H., 2013. Landslides Triggered by Slipping-Fault-Generated Earthquake on a Plateau: An Example of the 14 April 2010, *M*s 7.1, Yushu, China Earthquake. *Landslides*, 10(4): 421–431. doi:10.1007/s10346-012-0340-x

Xu, C., Xu, X. W., Shyu, J. B. H., 2015. Database and Spatial Distribution of Landslides Triggered by the Lushan, China *M*w 6.6 Earthquake of 20 April 2013. *Geomorphology*, 248: 77–92. doi:10.1016/j.geomorph.2015.07.002

Xu, C., Xu, X. W., 2014. Statistical Analysis of Landslides Caused by the M_w 6.9 Yushu, China, Earthquake of April 14, 2010. *Natural Hazards*, 72(2): 871–893. doi:10.1007/s11069-014-1038-2

Xu, C., Xu, X. W., Yao, X., et al., 2014. Three (Nearly) Complete Inventories of Landslides Triggered by the May 12, 2008 Wenchuan M_w 7.9 Earthquake of China and Their Spatial Distribution Statistical Analysis. *Landslides*, 11(3): 441–461. doi:10.1007/s10346-013-0404-6

Xu, X., Zhang, H., Deng, Q., 1988. The Paleoearthquake Traces on Huashan Front Fault Zone in Weihe Basin and Its Earthquake Intervals. *Seismology and Geology*, 10: 206 (in Chinese with English Abstract)

Yin, G. M., Lu, Y. C., Zhao, H., et al., 2001. The Tectonic Uplift of the Hua Shan in the Cenozoic. *Chinese Science Bulletin*, 46(19): 1665–1668. doi:10.1007/bf02900632

Yuan, T., Feng, X., 2010. The 1556 Huaxian Great Earthquake. Seismological Press, Beijing. 386 (in Chinese)

Zhang, D. X., Wang, G. H., 2007. Study of the 1920 Haiyuan Earthquake-Induced Landslides in Loess (China). *Engineering Geology*, 94(1/2): 76–88. doi:10.1016/j.enggeo.2007.07.007

Zhang, Y. Q., Mercier, J. L., Vergély, P., 1998. Extension in the Graben Systems around the Ordos (China), and Its Contribution to the Extrusion Tectonics of South China with Respect to Gobi-Mongolia. *Tectonophysics*, 285(1/2): 41–75. doi:10.1016/s0040-1951(97)00170-4

Zhang, A. L., Yang, Z. T., Zhong, J., et al., 1995. Characteristics of Late Quaternary Activity along the Southern Border Fault Zone of Weihe Graben Basin. *Quaternary International*, 25: 25–31. doi:10.1016/1040-6182(94)p3715-k

Zhou, Q., 2010. Ancient Landslide at the Pediment of the Qinling Mountains near Lianhuasi, Hua County, Shaanxi Province. *Journal of Shaanxi Institute of Education*, 26: 86–99 (in Chinese with English Abstract)